

Synthesis and Reactivity toward H₂ of (η⁵-C₅Me₅)Rh(III) Complexes with Bulky Aminopyridinate Ligands

Ana Zamorano, Nuria Rendón, José E. V. Valpuesta, Eleuterio Álvarez, and Ernesto Carmona**

Instituto de Investigaciones Químicas (IIQ) Departamento de Química Inorgánica and Centro de Innovación en Química Avanzada (ORFEO-CINQA)

Consejo Superior de Investigaciones Científicas (CSIC) and Universidad de Sevilla

Av. Américo Vespucio 49, Isla de la Cartuja, 41092 Sevilla (Spain)

Fax: (+34)954460565

E-mail: nuria@iiq.csic.es (N. R.), guzman@us.es (E. C.)

ABSTRACT. Electrophilic, cationic Rh(III) complexes of composition [(η⁵-C₅Me₅)Rh(Ap)]⁺, (**1**⁺), were prepared by reaction of [(η⁵-C₅Me₅)RhCl₂]₂ and LiAp (Ap = aminopyridinate ligand) followed by chloride abstraction with NaBA_{rF} (BA_{rF} = B[3,5-(CF₃)₂C₆H₃]₄). Reactions of

cations $\mathbf{1}^+$ with different Lewis bases (e. g. NH_3 , 4-dimethylaminopyridine or CNXyl) led in general to mono-adducts $\mathbf{1}\cdot\text{L}^+$ ($\text{L} = \text{Lewis base}$; $\text{Xyl} = 2,6\text{-Me}_2\text{C}_6\text{H}_3$) but carbon monoxide provided carbonyl-carbamoyl complexes $\mathbf{1}\cdot(\text{CO})_2^+$ as a result of metal coordination and formal insertion of CO into the $\text{Rh}\text{---}\text{N}_{\text{amido}}$ bond of complexes $\mathbf{1}^+$. Arguably, the most relevant observation reported in this study stemmed from the reactions of complexes $\mathbf{1}^+$ with H_2 . ^1H NMR analyses of the reactions demonstrated a H_2 -catalyzed isomerization of the aminopyridinate ligand in cations $\mathbf{1}^+$ from the ordinary $\kappa^2\text{-}N,N'$ -coordination to a very uncommon, formally tridentate $\kappa\text{-}N,\eta^3$ -pseudo-allyl bonding mode (complexes $\mathbf{3}^+$) following benzylic C—H activation within the xylyl substituent of the pyridinic ring of the aminopyridinate ligand. The isomerization entailed in addition H—H and N—H bond activation and mimicked previous findings with the analogous iridium complexes. However, in dissimilarity with iridium, rhodium complexes $\mathbf{1}^+$ reacted stoichiometrically at 20 °C with excess H_2 . The transformations resulted in the hydrogenation of the C_5Me_5 and Ap ligands with concurrent reduction to Rh(I), and yielded complexes $[(\eta^4\text{-C}_5\text{Me}_5\text{H})\text{Rh}(\eta^6\text{-ApH})]^+$, ($\mathbf{2}^+$), in which the pyridinic xylyl substituent is η^6 -bonded to the rhodium(I) centre. New compounds reported were characterized by microanalysis and NMR spectroscopy. Representative complexes were additionally investigated by X-ray crystallography.

INTRODUCTION

Organometallic compounds of rhodium and iridium that contain a $(\eta^5\text{-C}_5\text{Me}_5)\text{M(III)}$ fragment have been extensively investigated because of their capacity to participate in a wide range of chemical transformations.¹⁻⁶ Many of these complexes can be readily prepared from corresponding $(\text{C}_5\text{Me}_5)\text{M}$ halides⁷ by displacement reactions that utilize a variety of inorganic, organic and organometallic reagents.

A main, broad area of research that makes ample use of these complexes is the activation of C—H, H—H and other element-hydrogen bonds. Lately, our group has studied the reactivity of compounds of this type that contain a cyclometallated phosphine ligand, P[^]C.⁸ More recently, chelating, also monanionic, cyclometallated C[^]N and aminopyridinate⁹ (N[^]N) ligands have also been incorporated into $(\eta^5\text{-C}_5\text{Me}_5)\text{Ir(III)}$ structures. For instance, bulky aminopyridinate ligands (in shorthand notation represented from now on as Ap) have produced five-coordinate $[(\eta^5\text{-C}_5\text{Me}_5)\text{Ir(Ap)}]^+$ complexes¹⁰ in which the amido nitrogen atom acts as a π -donor to compensate the electronic unsaturation of the Ir(III) centre (an η^5 -cyclopentadienyl ligand is regarded to occupy three coordination sites).

During studies on the reactivity of these $[(\eta^5\text{-C}_5\text{Me}_5)\text{Ir(Ap)}]^+$ complexes we found that H₂ catalyzed a reversible isomerization of the coordinated Ap ligand, from its common κ^2, N, N' -coordination to a novel κ, N, η^3 -pseudo-allylic binding (structures **I** and **II** respectively in Figure 1A) in a process that entailed the reversible activation of H—H, C—H and N—H bonds.¹⁰ We therefore deemed of interest to prepare the rhodium complexes analogues and to study their reactivity toward dihydrogen. Here we report the results of this work that has allowed for the isolation and structural characterization of neutral and cationic rhodium complexes, $[(\eta^5\text{-$

$C_5Me_5Rh(Ap)Cl$ (**1·Cl**), and $[(\eta^5-C_5Me_5)Rh(Ap)]^+$ (**1**⁺), respectively (the latter isolated as BAr_F^- salts, where BAr_F stands for $B[(3,5-(CF_3)_2C_6H_3)_4]$ for the aminopyridinate groups labelled **a-d** in Figure 1A. Somewhat unexpectedly, and in marked contrast with the analogous iridium complexes the reaction of cations **1a**⁺-**1d**⁺ with H_2 provided only minor amounts of the isomeric complexes **3**⁺, with structure of type **II** in Figure 1. These complexes could not be isolated, but were structurally characterized in solution by NMR spectroscopy. The main products of the hydrogenation reactions were instead cationic Rh(I) complexes **2**⁺, with structure **III** (Figure 1B) that possess neutral pentamethylcyclopentadiene, C_5Me_5H , and aminopyridine, ApH , ligands with η^4 - and η^6 -coordination, respectively, in the latter case implicating the pyridine aryl substituent.

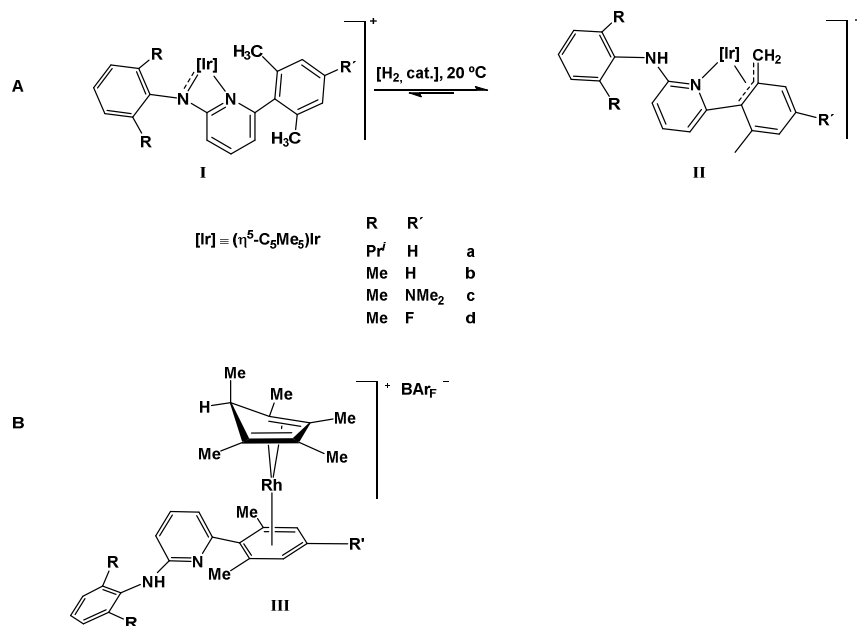
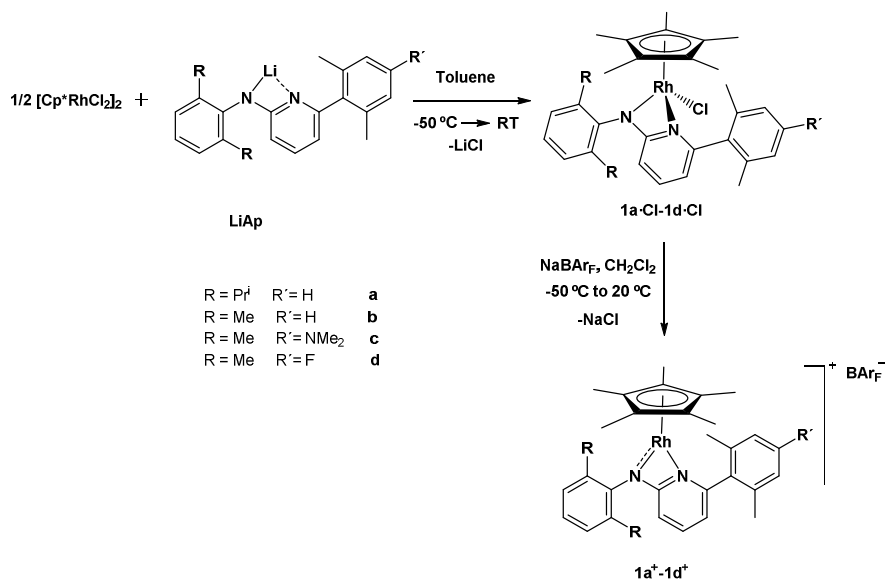


Figure 1. A: H_2 -catalyzed isomerization of aminopyridinate ligands in $[(\eta^5-C_5Me_5)Ir(Ap)]^+$ complexes (see reference 10). **B:** Main Rh(I) products resulting from the reactions of compounds $[(\eta^5-C_5Me_5)Rh(Ap)]^+$ with H_2 . Rh complexes with structure of type **II** were also detected and

were characterized by NMR studies (see below). The four Ap ligands labelled **a-d** were employed for both this work and that reported in reference 10a.

RESULTS AND DISCUSSION

Similarly to the iridium complexes analogues¹⁰ the targeted rhodium aminopyridinate derivatives were prepared by the low-temperature reaction of $[(\eta^5\text{-C}_5\text{Me}_5)\text{RhCl}_2]_2$ and the corresponding lithium aminopyridinate, LiAp (Scheme 1). The reactions yielded the expected neutral $[(\eta^5\text{-C}_5\text{Me}_5)\text{Rh}(\text{Ap})\text{Cl}]$ complexes, **1a·Cl-1d·Cl**, that were readily converted into the desired cationic species **1a⁺-1d⁺** upon treatment with NaBAR_F.



Scheme 1. Synthesis of neutral and cationic rhodium aminopyridinate complexes of the $(\eta^5\text{-C}_5\text{Me}_5)\text{Rh(III)}$ fragment.

The chlorides **1a**·Cl-**1d**·Cl were isolated as reddish crystalline solids. In contrast, both solution and solid samples of the **1a**⁺-**1d**⁺ cations have a characteristic dark green, almost black, colour. This is due to ligand-to-metal charge transfer π -d electronic transitions commonly encountered in complexes of this kind, in which the amido functionality exhibits a σ - and π - donor coordination behavior.¹¹ The new compounds were characterized by analytical techniques and by NMR spectroscopy (see the Experimental Section and the accompanying Supporting Information, SI). In addition, two neutral complexes, namely **1a**·Cl and **1b**·Cl, and the cationic derivatives **1b**⁺, **1c**⁺ and **1d**⁺ were further analyzed by X-ray crystallography. Members of these series were found to have similar structures. Therefore, only the molecular structures of **1b**·Cl and **1b**⁺ are depicted in Figure 2, whereas the others can be found in the SI (Figures S1 to S5).

The aminopyridinate ligand of both the neutral and the cationic complexes exhibits its classical bidentate coordination despite the strain it creates within the four-member $\overline{\text{Rh-N-C-N}}$ ring. This can be seen in the small N—Rh—N bite angle of *ca.* 62° found for the neutral complexes, that increases slightly in the five-coordinate cations **1**⁺ (to *ca.* 64.5° in **1b**⁺). In the neutral complexes the Rh—N_{py} and Rh—N_{amido} bonds have similar lengths, with the former being, as expected,

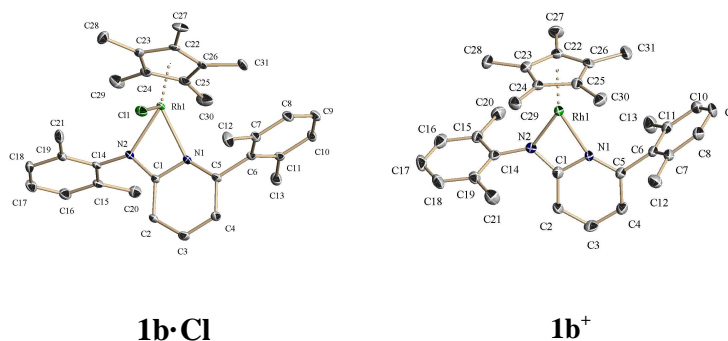
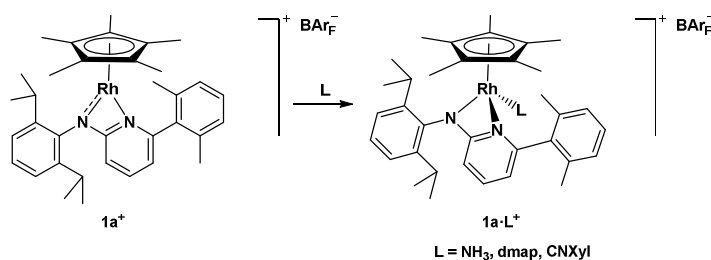


Figure 2. X-ray structure of complexes **1b**·Cl and **1b**⁺ (thermal ellipsoids set at 30% probability and

anions omitted for clarity). Selected bond lengths (Angstroms) and angles (degrees) for **1b·Cl**: Rh(1)–N(2) 2.113(3), Rh(1)–N(1) 2.162(3), Rh(1)–Cl(1) 2.3892(10), Rh(1)–C(22) 2.170(4), Rh(1)–C(23) 2.116(4), Rh(1)–C(24) 2.146(4), Rh(1)–C(25) 2.145(4), Rh(1)–C(26) 2.175(4), N(2)–Rh(1)–Cl(1) 88.91(9), N(1)–Rh(1)–Cl(1) 85.95(9), N(2)–Rh(1)–N(1) 62.05(12), C(1)–N(2)–Rh(1) 95.8(2), C(1)–N(1)–Rh(1) 92.3(2), N(2)–C(1)–N(1) 109.4(3). Selected bond lengths (Angstroms) and angles (degrees) for **1b⁺**: Rh(1)–N(1) 2.135(3), Rh(1)–C(24) 2.139(4), Rh(1)–N(2) 1.981(4), Rh(1)–C(25) 2.156(4), Rh(1)–C(22) 2.134(4), Rh(1)–C(26) 2.185(4), Rh(1)–C(23) 2.129(4), N(2)–Rh(1)–N(1) 64.51(14), C(1)–N(1)–Rh(1) 90.4(2), C(1)–N(2)–Rh(1) 97.4(3), N(2)–C(1)–N(1) 106.6(3).

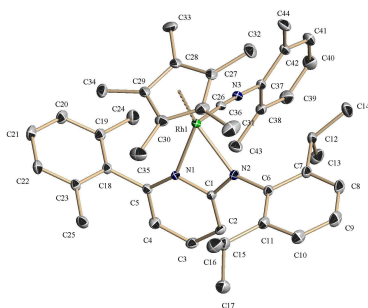
moderately longer than the latter (*ca.* 2.16 and 2.11 Å, respectively). These metrics are nearly identical to those reported for the analogous iridium complexes¹⁰ and are also comparable to corresponding values in a heterobinuclear Rh/Nd aminopyridinate complex.¹² At variance with these observations, the partial multiple character of the Rh—N_{amido} bond in the five-coordinated cations **1⁺** causes this bond to have a length significantly shorter (*ca.* 1.98 Å) than the Rh—N_{py} bond (2.14 Å). Once more, these structural parameters match closely those reported for somewhat related compounds with chelating monoanionic N^N ligands.^{10,11a,11c,13-17}

The five-coordinate Rh(III) center of cationic complexes **1⁺** exhibited Lewis acidity, as evidenced by the facile reaction of **1a⁺** with ammonia, 4-dimethylaminopyridine (dmap) and 2,6-dimethylphenyl isocyanide, CNXyl (Scheme 2). The reactions occurred almost instantaneously and were accompanied by a colour change from dark green to red-orange, indicative of the loss



Scheme 2. Lewis acid reactivity of the five-coordinate cationic complex $1a^+$.

of the π -component of the Rh—N_{amido} bond. The resulting adducts $1a \cdot L^+$ present spectroscopic properties similar to those of the analogous iridium complexes¹⁰ (see Experimental Section and SI). In particular, $1a \cdot CNXyl^+$ features $\bar{\nu}(CN)$ at 2160 cm^{-1} , i. e. some 45 cm^{-1} higher than for the free isocyanide. As for the analogous iridium adduct,¹⁰ this shift denotes that the CNXyl ligand behaves in this compound solely as a σ -donor. X-ray data for $1a \cdot CNXyl^+$ (Figure 3) are also alike those obtained for the iridium adduct analogue.¹⁰

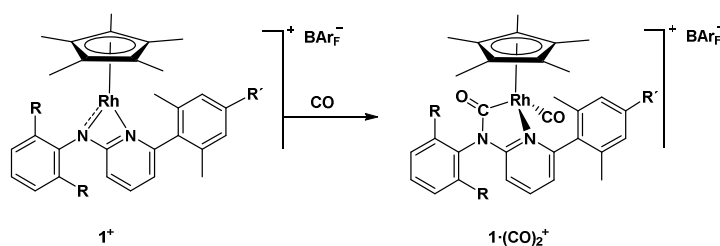


$1a \cdot CNXyl^+$

Figure 3. X-ray structure of complex $1a \cdot CNXyl^+$ (30% ellipsoids, H atoms and anion omitted for clarity). Selected bond lengths (Angstroms) and angles (degrees): Rh(1)—N(1) 2.1573(18), Rh(1)—N(2) 2.1172(19), Rh(1)—C(36) 1.989(2), C(36)—N(3) 1.156(3), Rh(1)—C(26) 2.180(3), Rh(1)—C(27) 2.144(3), Rh(1)—C(28) 2.178(2), Rh(1)—C(29) 2.193(2), Rh(1)—C(30) 2.180(3), C(36)-Rh(1)-N(1) 85.35(8), Rh(1)-N(2)-C(1) 95.37(13), C(36)-Rh(1)-N(2) 87.45(9), Rh(1)-N(1)-C(1) 92.47(13), N(1)-Rh(1)-N(2) 61.91(7), N(1)-C(1)-N(2) 109.19(19).

Interestingly, acetonitrile formed a bis(adduct) in which the aminopyridinate ligand is bonded to rhodium exclusively through the N_{amido} atom, $[(\eta^5\text{-C}_5\text{Me}_5)\text{Rh}(\kappa^1\text{-Ap})(\text{NCMe})_2]^+$, $\mathbf{1a}\cdot(\text{NCMe})_2^+$ (only the mono-adduct $[(\eta^5\text{-C}_5\text{Me}_5)\text{Ir}(\kappa^2\text{-Ap})(\text{NCMe})]^+$ was detected for iridium¹⁰). The existence of a symmetry plane simplifies considerably the ¹H and ¹³C{¹H} NMR spectra of this complex. For instance, only one septet (3.22 ppm) and two doublets (1.08 and 1.35 ppm; ³J_{HH} = 7.0 Hz) were recorded for the *i*-Pr substituents of the N_{amido} aryl group and one singlet (2.26 ppm) for the methyl protons of the pyridine xylyl substituent.

Also in dissimilarity with the analogous iridium system, complexes $\mathbf{1}^+$ reacted with CO with incorporation of two molecules of CO (Scheme 3) and formation of the new compounds



Scheme 3. The reaction of complexes $\mathbf{1}^+$ with carbon monoxide.

$\mathbf{1}\cdot(\text{CO})_2^+$ that contain a terminal carbonyl ($\bar{\nu}(\text{CO}) = 2070 \text{ cm}^{-1}$) and a carbamoyl unit that is part of a five-member $\overline{\text{Rh-N-C-N-C(O)}}$ ring ($\bar{\nu}(\text{CO}) = 1690 \text{ cm}^{-1}$, data for $\mathbf{1a}\cdot(\text{CO})_2^+$). Comparable reactivity has been disclosed for ruthenium^{14a-d} and iridium.^{14e} In the ¹³C{¹H} NMR spectrum of these compounds the Rh—CO resonance appears at about 187 ppm (¹J_{CRh} ca. 75 Hz) while the Rh—C(O)N functionality can be found nearby (~188 ppm) also in the form of a doublet (¹J_{CRh} of

ca. 30 Hz). Figure 4 contains ORTEP drawings of the molecular structure of **1a**•(CO)₂⁺ and **1b**•(CO)₂⁺.

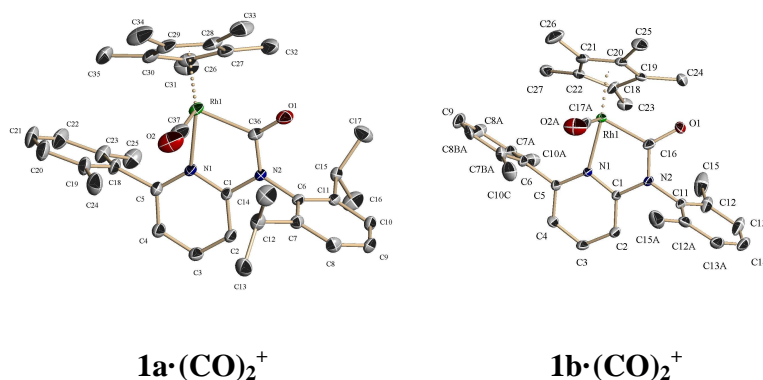


Figure 4. ORTEP view of the molecular structure of complexes **1a**•(CO)₂⁺ and **1b**•(CO)₂⁺ (30% ellipsoids, H atoms and anions omitted for clarity). Selected bond lengths (Angstroms) and angles (degrees) for **1a**•(CO)₂⁺: Rh(1)—N(1) 2.170(3), Rh(1)—C(26) 2.251(4), Rh(1)—C(37) 1.921(5), Rh(1)—C(27) 2.226(4), O(2)—C(37) 1.133(5), Rh(1)—C(28) 2.163(4), Rh(1)—C(36) 2.033(4), Rh(1)—C(29) 2.231(4), O(1)—C(36) 1.206(5), Rh(1)—C(30) 2.309(4), C(37)-Rh(1)-N(1) 93.29(16), Rh(1)-C(36)-N(2) 113.0(2), C(37)-Rh(1)-C(36) 87.00(18), Rh(1)-N(1)-C(1) 111.2(2), N(1)-Rh(1)-C(36) 79.28(12), N(1)-C(1)-N(2) 116.9(3). Selected bond lengths (Angstroms) and angles (degrees) for **1b**•(CO)₂⁺: Rh(1)—N(1) 2.146(4), Rh(1)—C(18) 2.20(3), Rh(1)—C(17) 1.95(3), Rh(1)—C(19) 2.241(7), O(2)—C(17) 1.05(3), Rh(1)—C(20) 2.160(7), Rh(1)—C(16) 2.000(6), Rh(1)—C(21) 2.262(7), O(1)—C(16) 1.270(7), Rh(1)—C(22) 2.330(7), C(17)-Rh(1)-N(1) 97.8(9), N(2)-C(16)-Rh(1) 112.9(4), C(17)-Rh(1)-C(16) 92.9(6), C(1)-N(1)-Rh(1) 111.2(3), C(16)-Rh(1)-N(1) 79.98(19), N(1)-C(1)-N(2) 116.7(4).

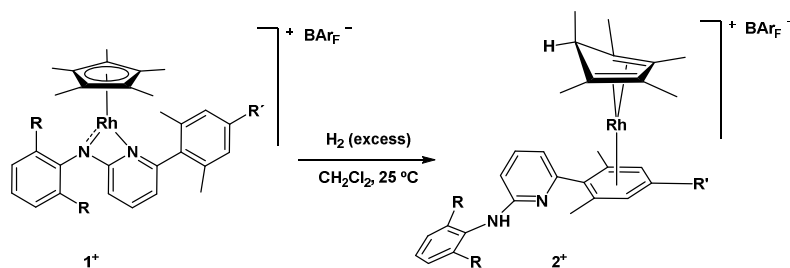
As expected, they display noticeable differences in the lengths of the two rhodium-carbonyl group bonds (*ca.* 1.92 Å for Rh—CO and 2.02 Å for the Rh—carbamoyl terminus). Corresponding C—O distances are also different (*ca.* 1.10 and 1.23 Å, respectively) as foreseen

for essentially triple and double C—O bonds, and sp- and sp²-hybridized carbon atoms, respectively.

Reactivity of complexes **1**⁺ toward H₂

Amido derivatives of ($\eta^5\text{C}_5\text{Me}_5$)M fragments (M = group 8 and 9 metals), particularly those that incorporate a chelating amine-amido ligand, have a rich chemistry that permits their utilization in the activation of H₂ and other small molecules. As a matter of fact, many complexes of this type behave as bifunctional M/N_{amido} catalysts for hydrogen transfer, heterolytic hydrogenations and even C—C bond forming reactions.^{6,11,12,15,16}

Contrary to the reactions of the homologous iridium cations [$(\eta^5\text{-C}_5\text{Me}_5)\text{Ir}(\text{Ap})$]⁺ with H₂, that under appropriate conditions yielded exclusively equilibrium mixtures of the isomeric structures **I** and **II** represented in Figure 1A, the interaction of the rhodium species **1**⁺ with H₂ (1 bar, an excess) turned out to proceed through a seemingly more complex course, because it provided as principal reaction products the cationic Rh(I) complexes **2**⁺ represented in Scheme 4 (see also structure **III** in Figure 1B). The new complexes **2**⁺ contain neutral pentamethylcyclopentadiene (C₅Me₅H) and aminopyridine (ApH) ligands coordinated in η^4 -diene and η^6 -arene fashions, respectively. Thus, in a formal sense the monoanionic C₅Me₅ and



Scheme 4. Generation of the Rh(I) complexes 2⁺ by reaction the Rh(III) precursors 1⁺ and H₂.

Ap ligands of complexes 1⁺ underwent hydrogenation to C₅Me₅H and ApH, respectively, with concomitant reduction of Rh(III) to Rh(I). For all complexes 1⁺ the reactions were essentially quantitative, although partial decomposition of complexes 2⁺ by action of the solvent (CH₂Cl₂) could not be avoided (see below).

The Rh(I) complexes [2]BAr_F proved to be air stable in the solid state but decomposed in solution in contact with air. Under an inert atmosphere their CH₂Cl₂ solutions decomposed partially to give the known¹⁸ binuclear compound [(η⁵C₅Me₅)₂Rh₂(μ-Cl)₃][BAr_F], whose chloride ligands originate from the solvent through an undisclosed, probably radical mechanism. It seems that decomposition is triggered by arene dissociation, as hinted by the comparatively faster decomposition of complex 2d⁺ that contains a fluoro-substituted η⁶-arene ring. The molecular complexity of cations 2⁺ was unveiled by an X-ray diffraction analysis of 2b⁺ and was subsequently confirmed by solution NMR studies.

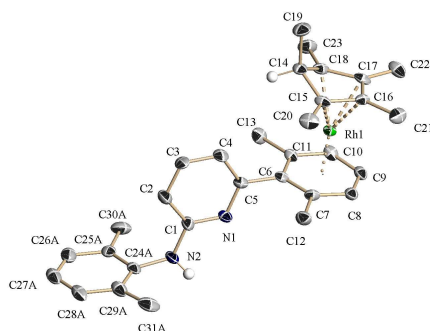


Figure 5. ORTEP view of the molecular structure of complex **2b⁺** (30% ellipsoids, H atoms and anion omitted for clarity). Selected bond lengths (Angstroms) and angles (degrees): Rh(1)–C(6) 2.341(7), Rh(1)–C(17) 2.113(8), Rh(1)–C(7) 2.300(8), Rh(1)–C(18) 2.140(8), Rh(1)–C(8) 2.306(8), C(14)–C(15) 1.496(12), Rh(1)–C(9) 2.317(9), C(15)–C(16) 1.436(12), Rh(1)–C(10) 2.260(8), C(16)–C(17) 1.438(12), Rh(1)–C(11) 2.318(7), C(17)–C(18) 1.485(13), Rh(1)–C(15) 2.161(8), C(14)–C(18) 1.489(13), Rh(1)–C(16) 2.136(7), C(16)–C(15)–Rh(1) 69.5(4), C(16)–Rh(1)–C(15) 39.0(3), C(17)–C(16)–Rh(1) 69.4(4), C(17)–Rh(1)–C(16) 39.6(3), C(18)–C(17)–Rh(1) 70.5(5), C(17)–Rh(1)–C(18) 40.9(4), C(14)–C(18)–Rh(1) 93.6(5), N(1)–C(5)–C(6) 114.7(7), C(14)–C(15)–Rh(1) 92.5(5), N(1)–C(1)–N(2) 117.1(8).

Figure 5 depicts the molecular structure of the cationic complex **2b⁺**. As can be seen, the Rh(I) center is bonded to the C₅Me₅H ring through the C15–C16 and C17–C18 double bonds, with an average Rh—C distance of 2.14 Å (comparable to the Rh—C₅Me₅ distances in the parent complex **1b⁺**, that vary between 2.12 and 2.18 Å). The non-coordinated sp³-hybridized carbon atom C14 features *endo*-H and *exo*-Me substituents, suggesting that complexes **2⁺** form by intramolecular H transfer from Rh to C₅Me₅ in a putative, non-detected (η⁵-C₅Me₅)Rh(III) hydride intermediate (*vide infra*).^{19,20} This carbon atom C14 deviates considerably from the plane defined by the other four, sp²-hybridized carbon atoms C15–C18. Indeed, the dihedral angle between the latter plane and that defined by C15, C14 and C18 is of 34.53 °, a value analogous to

those found in related complexes.²¹ The coordination of rhodium is completed by an η^6 -interaction with the 2,6-Me₂C₆H₃ aryl ring bound to the pyridinic unit of the neutral aminopyridine ligand. The metal-arene electronic interaction is characterized by relatively long Rh—C bonds, the lengths of which vary between *ca.* 2.26 and 2.34 Å. These separations are similar to, albeit somewhat longer than those reported for other Rh(I)-arene complexes.²² Transition metal compounds with an η^4 -C₅Me₅H ligand that have been authenticated by X-ray crystallography are scarce but some examples are known.^{19a,23}

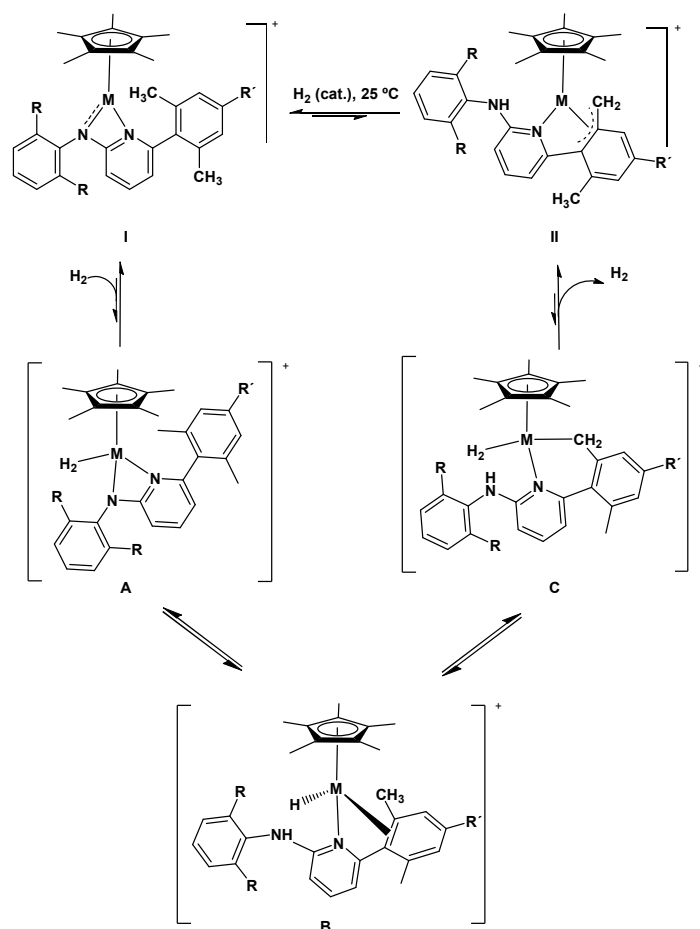
NMR data for the new complexes **2**⁺ are in excellent agreement with the solid-state structure ascertained for **2b**⁺ and discussed in the anterior paragraph. Taking the latter species as a representative example, the most noticeable ¹H NMR changes that accompany the dihydrogen-induced transformation of complex **1b**⁺ into **2b**⁺ are the disappearance of the resonance centered at 1.29 ppm (relative intensity 15 H) attributable to the η^5 -C₅Me₅ ligand of **1b**⁺ and the emergence of a set of signals that can be assigned with safety to a neutral molecule of C₅Me₅H with η^4 -coordination to rhodium. These are: (i) two singlets with chemical shifts 1.95 and 1.32 ppm, each corresponding to two chemically equivalent =C(Me) groups (hence, each with relative intensity equivalent to 6 H); (ii) one doublet (0.43 ppm; ³J_{HH} = 6.5 Hz, 3H); (iii) and a quartet (2.78 ppm, ³J_{HH} = 6.5 Hz, 1 H). The latter resonances are assignable to the methyl and methine protons of the C(H)Me) unit, respectively.

Additionally, it is worth mentioning that the neutral aminopyridine ligand of **2b**⁺ is also responsible for a broad singlet centered at δ 5.93 due to the NH proton. Moreover, the CH protons of the rhodium-bound η^6 -2,6-Me₂C₆H₃ ring are shifted toward lower frequencies by nearly 1 ppm relative to corresponding signals of the non-coordinated xylyl substituents. These

protons resonate as a triplet and a doublet with δ 6.39 (1 H; $^3J_{\text{HH}} \sim 6.5$ Hz) and 6.01 (2 H; $^3J_{\text{HH}} \sim 6.5$ Hz).

^1H NMR monitoring of the reactions of complexes $\mathbf{1}^+$ with H_2 provided useful supplementary information. Firstly, it revealed the formation of small amounts of the expected (by similarity with the iridium system analogue¹⁰) Rh(III) complexes, $\mathbf{3}^+$, which are isomers of cations $\mathbf{1}^+$ with a structure of type **II** in Figure 1A. Thus, using *ca.* 20-60 mol% concentrations of H_2 , complexes $\mathbf{3}^+$ formed in about 5-20% quantities with the exception of the fluoro-containing cation $\mathbf{3d}^+$ that resulted in approximately 50% yield by ^1H NMR (see below). Under these conditions, scant proportions of the Rh(I) derivatives $\mathbf{2}^+$ and the decomposition product $[(\eta^5\text{C}_5\text{Me}_5)_2\text{Rh}_2(\mu\text{-Cl})_3][\text{BAr}_\text{F}]$ were also detected. Evidently, the $\mathbf{1}^+$ -to- $\mathbf{3}^+$ rearrangement required H—H and C—H bond cleavage as well as N—H bond formation. In addition, complexes $\mathbf{3}^+$ were also detected in the reactions of $\mathbf{1}^+$ with an excess of H_2 and were found to disappear in favour of the Rh(I) derivatives $\mathbf{2}^+$. However, their back conversion to corresponding isomers $\mathbf{1}^+$ could not be observed.

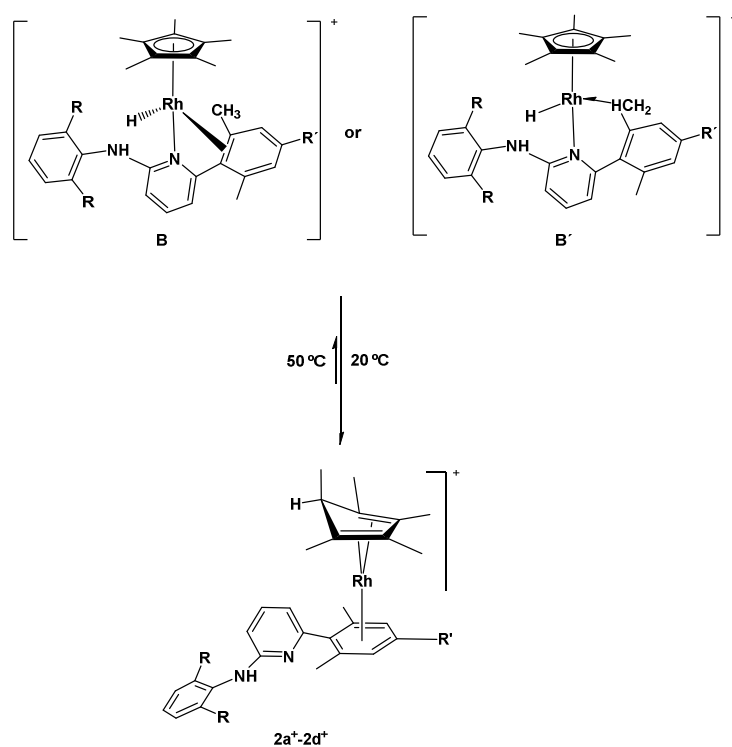
Scheme 5 shows the general mechanism for the H_2 -catalyzed interconversion of aminopyridinate isomeric structures **I** and **II** that was advanced for iridium complexes with the



Scheme 5. General mechanism for the interconversion of rhodium and iridium isomeric complexes with structures I and II in the presence of H_2 .

support of experimental and computational studies.¹⁰ Even if it is likely that related equilibria exist between the Rh(III) complexes 1^+ and 3^+ , unequivocal proof for their operation could not be gathered. Probably this is due to the formation of complexes 3^+ only in minute concentrations and above all to the appearing of the Rh(I) complexes 2^+ (which are actually unknown for iridium) as the main reaction products. Besides, partial decomposition of the latter to $[(\eta^5-$

$C_5Me_5)_2Rh_2(\mu-Cl)_3][BAR_F]$ introduced additional complexity into the reaction manifold. For rhodium, it appears likely that complexes 2^+ derive from a Rh(III) hydride intermediate with structure alike **B**, although an alternative structure **B'** (Scheme 6) in which a δ -agostic interaction replaces the η^2 -arene binding seems also reasonable. The latter hypothesis finds strong support in the observation of a related, also cationic, hydride agostic structure derived from a (η^5 - C_5Me_5)Rh(III) fragment and a metallated $PMeXyl_2$ ligand.^{8b} Regardless of the precise



Scheme 6. Proposed formation of the Rh(I) complexes $2a^+-2d^+$ from intermediate **B** or **B'**.

nature of this hydride intermediate, a reductive coupling step involving its Rh—H and Rh—C₅Me₅ functionalities, along with a conformational change aimed to establish the Rh(I)-η⁶-arene bonding interaction, would account for the formation of complexes **2**⁺.

It is important to note that as indicated in Schemes 5 and 6, the formation of complexes **2**⁺ could be reverted. In this manner larger amounts of complexes **3**⁺ (structure of type **II** in Scheme 5) were generated (see the Experimental Section) permitting their complete characterization by NMR studies. Thus, when CD₂Cl₂ solutions of previously isolated samples of complexes **2**⁺ were heated at 50 °C in an NMR tube, the corresponding isomers **3**⁺ were readily identified. Partial decomposition to the chloride-bridged dinuclear compound [(η⁵-C₅Me₅)₂Rh₂(μ-Cl)₃][BAR_F] took also place, but under these conditions the back conversion of **3**⁺ into the isomeric complexes **1**⁺ could not be observed. In the absence of theoretical calculations we can offer no rigorous explanation for the lack of observation of this isomer. However, it is possible that, as for iridium, the thermodynamics favour isomers **3**⁺ relative to **1**⁺, making the back **3**⁺-to-**1**⁺ conversion slower. This, added to the perturbation introduced in the reaction system by the Rh(I) complexes **2**⁺, and by their relatively easy decomposition to [(η⁵-C₅Me₅)₂Rh₂(μ-Cl)₃][BAR_F], could justify our failure to observe complexes **1**⁺ under these conditions.

Another relevant piece of knowledge provided by the ¹H NMR monitoring of the reactions of complexes **1**⁺ with H₂ is the facility of formation of complexes **2**⁺ under the conditions of Scheme 4. Complexes **1a**⁺ and **1b**⁺ differ in the nature of the N_{amido} aryl substituent, viz 2,6-Pr₂ⁱC₆H₃ and 2,6-Me₂C₆H₃, respectively (See Figure 1A). It was found that quantitative formation of **2a**⁺ (≥ 95% by ¹H NMR) required 6 h, whereas that **2b**⁺ needed only 1h. In

agreement with the isomerization mechanism represented in Scheme 5, this difference reflects, most probably, the steric hindrance exerted by the *i*-Pr substituents of **1a**⁺ to coordination of H₂ to form intermediate **A**. On the other hand, complexes **1b**⁺, **1c**⁺ and **1d**⁺ are very similar but may be distinguished thanks to the different R' group in the 4-position of the aryl substituents of the pyridine ring (H for **1b**⁺, NMe₂ in **1c**⁺ and F in the case of **1d**⁺). As already mentioned, quantitative conversion into **2b**⁺ needed 1h, whereas for **2c**⁺ 3h were required. As for **2d**⁺, its formation was the fastest, with a 75 % yield after only 10 min. Higher yields of **2d**⁺ could not be reached due to its decomposition to $[(\eta^5\text{C}_5\text{Me}_5)_2\text{Rh}_2(\mu\text{-Cl})_3][\text{BAr}_\text{F}]$, probably facilitated by dissociation of the F-containing η^6 -arene ring. The above differences may arise from the facility with which the purported Rh(III) hydride intermediates with structure **B**, or **B'**, experience reductive coupling to the corresponding isomeric Rh(I) structures **2**⁺.

Before closing, some comments on the divergent behavior of the iridium and rhodium complexes of composition $[(\eta^5\text{-C}_5\text{Me}_5)\text{M}(\text{Ap})]^+$ in their reactions with H₂ appear appropriate. Firstly, reductive coupling and reductive elimination of M—H^{20,24} (or M—Me²⁵) and C₅Me₅ or other cyclopentadienyl ligands, have been observed for various transition metals, in some cases in a reversible manner.^{19,20,23,25} Secondly, the formation under mild conditions of the rhodium complexes **2**⁺ that, as already noted, are unknown for iridium, is, in almost all probability, a consequence of the easier reduction of Rh(III) to Rh(I) in comparison with the analogous Ir(III) to Ir(I) redox change. Such difference in the relative stability of metal oxidation states, not only in the +1 and +3 ones, but also in others, are commonly encountered in the chemistry of late transition elements, particularly of rhodium and iridium. For example, during studies on cyclometallations, Leong and co-workers obtained different types of products in the course of the reactions of the Rh and Ir $[(\eta^5\text{-C}_5\text{Me}_5)\text{MCl}_2]_2$ dimers with an anyline and a terminal alkyne, that

were explained by reason of the more difficult accessibility of the M(V) oxidation state for rhodium.²⁶ On a completely different topic, in recent studies of the double deprotonation of the bis(2-picoyl)amine ligand in Rh(I) and Ir(I) complexes, $[M(\text{bpa})(\text{cod})]^+$ (cod = 1,5-cyclooctadiene), Tejel, de Bruin, Ciriano and co-workers explained the observed thermodynamic differences in the products as arising from the lower stability of Ir(-1) in comparison with Rh(-1).^{17b} A last, truly remarkable example that implicates the +1 and +3 oxidation states was provided by Brookhart and co-workers, who took advantage of the ease of reduction of Rh(III) relative to Ir(III) to observe and characterize by solution NMR spectroscopy a relatively long-lived σ -methane complex of rhodium (I).²⁷

In summary, this contribution extends previous studies on the reactivity of cationic Ir(III) complexes of composition $[(\eta^5\text{-C}_5\text{Me}_5)\text{Rh}(\text{Ap})]^+$ with H_2 ¹⁰ to the rhodium analogues (complexes 1^+). For the two metals a dihydrogen-catalyzed isomerization of the aminopyridinate ligand from the common $\kappa^2\text{-N,N'}$ bidentate coordination to an unusual $\kappa\text{-N-}\eta^3$ -pseudo-allyl bonding mode (Rh complexes 3^+) has now been documented (Figure 1A), in a rearrangement that required H—H, C—H and N—H bond activation. However, while for iridium this was the principal chemical change observed,¹⁰ for rhodium a stoichiometric hydrogenation of the C_5Me_5 and aminopyridinate ligands to $\text{C}_5\text{Me}_5\text{H}$ and ApH , respectively, took place, with concomitant metal reduction to Rh(I) (complexes 2^+). This was demonstrated to be the main reaction path and occurred irreversibly at room temperature in the presence of an excess of H_2 . The dissimilar chemical behavior of the rhodium compounds relative to the iridium analogues is most likely due to more facile reduction of M(III) to M(I) for rhodium than for iridium.

EXPERIMENTAL SECTION

General Procedures: Microanalyses were performed by the Microanalytical Service of the Instituto de Investigaciones Químicas (Sevilla, Spain). Infrared spectra were obtained from Bruker Vector 22 spectrometer. The mass spectra were obtained at the Mass Spectroscopy Service of the University of Sevilla (CITIUS). The NMR instruments were Bruker DRX-500, DRX-400 and DPX-300 spectrometers. Spectra were referenced to external SiMe₄ (δ 0 ppm) using the residual protio solvent peaks as internal standards (¹H NMR experiments) or the characteristic resonances of the solvent nuclei (¹³C NMR experiments). Spectral assignments were made by routine one- and two-dimensional NMR experiments where appropriate. All manipulations were performed under dry, oxygen-free dinitrogen, following conventional Schlenk techniques. The crystal structures were determined in a Bruker-Nonius, X8Kappa diffractometer. Metal complex [Cp*RhCl₂]₂,^{7b} as well as NaBAR_F²⁸ were prepared as previously described. The lithium salt of the aminopyridinate ligands were prepared according to published procedures.^{9b} The ¹H and ¹³C{¹H} NMR spectral data for the BAR_F anion (BAR_F = B[3,5-(CF₃)₂C₆H₃]₄) in CD₂Cl₂ are identical for all complexes and therefore are not repeated below. ¹H NMR: δ 7.75 (s, 8 H, *o*-Ar), 7.58 (s, 4 H, *p*-Ar). ¹³C{¹H} NMR: δ 162.1 (q, ¹J_{CB} = 37 Hz, *ipso*-Ar), 135.3 (*o*-Ar), 129.2 (q, ²J_{CF} = 31 Hz, *m*-Ar), 124.9 (q, ¹J_{CF} = 273 Hz, CF₃), 117.8 (*p*-Ar).

Compound 1a·Cl. A toluene solution of the corresponding LiAp (240 mg, 0.66 mmoles; 2 mL) at -50 °C was added to a suspension of [Cp*RhCl₂]₂ (200 mg, 0.32 mmoles) in toluene at -50 °C. The resulting mixture was stirred, allowed to warm to room temperature and stirred for a further period of 5 h. The solution was filtered through celite and the solvent removed under reduced pressure. ¹H NMR analysis of the crude reaction mixture showed quantitative conversion into **1a·Cl**, which was crystallized from Et₂O-hexane mixtures at -23 °C. ¹H NMR (C₆D₆, 25 °C): δ =

7.32, 7.23, 7.21, (d, t, d, 1 H each, $^3J_{\text{HH}} \sim 7.5$ Hz, 3 CH_{Dipp}), 7.06, 7.02, 6.92 (t, d, d, 1 H each, $^3J_{\text{HH}} \sim 7.5$ Hz, 3 CH_{Xyl}), 6.65, 5.66, 5.42 (t, d, d, 1 H each, $^3J_{\text{HH}} \sim 7.5$ Hz, 3 CH_{Pyr}), 4.42, 3.53 (sept, 1 H each, $^3J_{\text{HH}} \sim 7.0$ Hz, 2 CH_{iPr}), 2.72, 2.21 (s, 3 H each, 2 Me_{Xyl}), 1.43, 1.35, 1.32, 1.23 (d, 3 H each, $^3J_{\text{HH}} \sim 7.0$ Hz, 4 Me_{iPr}), 1.03 (s, 15 H, 5 Me_{Cp^*}). $^{13}\text{C}\{^1\text{H}\}$ NMR (C_6D_6 , 25 °C): $\delta = 172.4, 157.4$ ($\text{C}_{\text{q-Pyr}}$), 148.0, 147.9, 139.6 ($\text{C}_{\text{q-Dipp}}$), 140.9, 138.7, 137.0 ($\text{C}_{\text{q-Xyl}}$), 136.8, 107.2, 106.5 (CH_{Pyr}), 128.0, 126.9 (2:1, CH_{Xyl}), 125.4, 124.3, 124.0 (CH_{Dipp}), 91.6 (d, $^1J_{\text{RhC}} = 8$ Hz, $\text{C}_{\text{q-Cp}^*}$), 28.3, 28.0 (CH_{iPr}), 26.9, 25.8, 25.0, 23.6 (Me_{iPr}), 22.1, 20.1 (Me_{Xyl}), 8.8 (Me_{Cp^*}). Anal. Calcd (%) for $\text{C}_{35}\text{H}_{44}\text{ClN}_2\text{Rh}$: C, 66.6; H, 7.0; N, 4.4. Found: C, 66.5; H, 7.2; N, 4.1.

Compounds 1b·Cl-1d·Cl: See the Supporting Information for synthetic details and characterization data.

Compound [1a]BAR_F. To a solution of **1a·Cl** (374 mg, 0.593 mmol) in CH_2Cl_2 (5 mL), NaBAR_F (524 mg, 0.593 mmol) in CH_2Cl_2 (3 mL) was added. Immediately, the colour of the solution turned from red to dark green as a consequence of the formation of the cationic complex. The resulting mixture was filtered through celite, evaporated to dryness and the residue washed with pentane, to yield quantitatively complex **[1a]BAR_F**. ^1H NMR (CD_2Cl_2 , 25 °C): $\delta = 7.30$ (m, 7 H, 1 CH_{Pyr} + 3 CH_{Xyl} + 3 CH_{Dipp}), 6.20, 5.16 (d, 1 H each, $^3J_{\text{HH}} \sim 7.5$ Hz, 2 CH_{Pyr}), 3.53 (sept, 2 H, $^3J_{\text{HH}} \sim 7.0$ Hz, 2 CH_{iPr}), 2.32 (s, 6 H, 2 Me_{Xyl}), 1.44, 1.14 (d, 6 H each, $^3J_{\text{HH}} \sim 7.0$ Hz, 4 Me_{iPr}), 1.32 (s, 15 H, 5 Me_{Cp^*}). $^{13}\text{C}\{^1\text{H}\}$ NMR (CD_2Cl_2 , 25 °C): $\delta = 179.9, 156.5$ ($\text{C}_{\text{q-Pyr}}$), 145.6, 137.0 (2:1, $\text{C}_{\text{q-Dipp}}$), 144.4, 116.3, 102.9 (CH_{Pyr}), 137.6, 135.7 (1:2 C, $\text{C}_{\text{q-Xyl}}$), 130.0, 128.5 (1:2, CH_{Xyl}), 128.0, 124.6 (1:2, CH_{Dipp}), 94.7 ($\text{C}_{\text{q-Cp}^*}$), 28.7 (CH_{iPr}), 25.2, 23.8 (Me_{iPr}), 20.2 (Me_{Xyl}), 9.5 (Me_{Cp^*}). Anal. Calcd (%) for $\text{C}_{67}\text{H}_{56}\text{BF}_{24}\text{N}_2\text{Rh}$: C, 54.2; H, 3.9; N, 1.9. Found: C, 54.2; H, 4.5; N, 1.5.

Compounds [1b]BAR_F-[1d]BAR_F: See the supporting Information for synthetic details and characterization data.

Compound [1a·NH₃]BAr_F. NH₃ (g) was bubbled through a solution of compound [1a]BAr_F (100 mg, 0.071 mmol) in CH₂Cl₂ (5 mL) for 5 min. During this period of time the colour of the solution changed from dark green to bright red. The resulting mixture was stirred for 30 minutes and the volatiles were then removed under reduced pressure. ¹H NMR analysis of the crude product revealed quantitative conversion into complex [1a·NH₃]BAr_F. ¹H NMR (CD₂Cl₂, 0 °C): δ = 7.25 (m, 7 H, 3 CH_{Xyl} + 3 CH_{Dipp} + 1 CH_{Pyr}), 6.11, 5.74 (d, 1 H each, ³J_{HH} ~ 7.5 Hz, 2 CH_{Pyr}), 3.10, 2.66 (br s, 1 H each, 2 CH_{iPr}), 2.44 (s, 3 H, NH₃), 2.20, 2.17 (s, 3 H each, 2 Me_{Xyl}), 1.32, 1.12, 1.02 (br s, 2:1:1, 4 Me_{iPr}), 1.25 (s, 15 H, 5 Me_{Cp*}). ¹³C{¹H} NMR (CD₂Cl₂, 0 °C): δ = 173.6, 156.8 (C_{q-Pyr}), 147.8, 143.7, 136.9 (br, C_{q-Dipp}), 138.9, 129.4, 125.9 (CH_{Xyl} + CH_{Dipp} + CH_{Pyr}), 138.5, 137.6, 133.9 (br, C_{q-Xyl}), 128.4, 127.9, 125.9, 123.3 (br, CH_{Dipp} + CH_{Xyl}), 110.3, 108.0 (CH_{Pyr}), 94.0 (d, ¹J_{CRh} = 8.2 Hz, C_{q-Cp*}), 29.4, 28.3 (CH_{iPr}), 26.0, 25.1, 24.0, 21.4 (Me_{iPr}), 20.7, 20.1 (Me_{Xyl}), 8.7 (CH_{Cp*}). Anal. Calcd (%) for C₆₇H₅₄BF₂₄N₃Rh: C, 54.5; H, 4.0; N, 2.8. Found: C, 54.5; H, 4.0; N, 2.7.

Adducts of complex **1a**⁺ with dmap, CNXyl and NCMe were prepared by a similar procedure (see SI).

Compound [1a·(CO)₂]BAr_F CO (g) was bubbled through a solution of compound [1a]BAr_F (100 mg, 0.071 mmol) in CH₂Cl₂ (5 mL) for 5 min. During this period of time the colour of the solution changed from dark green to yellow-orange. The resulting mixture was stirred for 3 h and the volatiles were then removed under reduced pressure. ¹H NMR analysis of the crude product revealed quantitative conversion into complex [1a·(CO)₂]BAr_F, which was crystallized from CH₂Cl₂-Et₂O-hexane mixtures at -23 °C. IR (Nujol): ν(CO) 2070, ν(CO_{amide}) 1690 cm⁻¹. ¹H NMR (CD₂Cl₂, 25 °C): δ = 7.78, 7.00, 6.51 (t, d, d, ³J_{HH} ~ 7.5 Hz, 3 CH_{Pyr}), 7.60, 7.40 (t, d, 1:2, ³J_{HH} ~ 7.5 Hz, 3 CH_{Dipp}), 7.43, 7.31, 7.27 (m, d, d, 1 H each, ³J_{HH} ~ 7.5 Hz, 3 CH_{Xyl}), 2.67, 2.32

(sept, 1 H each, $^3J_{\text{HH}} \sim 7.0$ Hz, 2 CH_{iPr}), 2.17, 2.16 (s, 3 H each, 2 Me_{Xyl}), 1.59 (s, 15 H, 5 Me_{Cp^*}), 1.26, 1.18, 1.12, 1.04 (d, 3 H each, $^3J_{\text{HH}} \sim 7.0$ Hz, 4 Me_{iPr}). $^{13}\text{C}\{^1\text{H}\}$ NMR (CD_2Cl_2 , 25 °C): $\delta = 188.4, 186.8$ (d, $^1J_{\text{CRh}} = 30$ Hz, $^1J_{\text{CRh}} = 75$ Hz, Rh-CON and Rh-CO, resp.), 160.2, 158.6 ($\text{C}_{\text{q-Pyr}}$), 146.2, 146.0 ($\text{C}_{\text{q-Dipp}}$), 141.4, 123.6, 111.0 (CH_{Pyr}), 138.6, 136.3, 133.2 ($\text{C}_{\text{q-Xyl}} + \text{C}_{\text{q-Dipp}}$), 137.2 ($\text{C}_{\text{q-Xyl}}$), 131.4, 125.8, 125.6 (CH_{Dipp}), 130.8, 129.4, 129.2 (CH_{Xyl}), 109.6 (d, $^1J_{\text{RhC}} = 5$ Hz, $\text{C}_{\text{q-Cp}^*}$), 30.0, 29.5 (CH_{iPr}), 24.3, 24.1, 23.9, 23.5 (Me_{iPr}), 22.1, 21.3 (Me_{Xyl}), 9.4 (Me_{Cp^*}). Anal. Calcd (%) for $\text{C}_{69}\text{H}_{56}\text{BF}_{24}\text{N}_2\text{O}_2\text{Rh}$: C, 54.7; H, 3.7; N, 1.8. Found: C, 54.8; H, 4.0; N, 1.8.

Related carbonyl derivatives of $\mathbf{1b}^+ - \mathbf{1d}^+$ were prepared by an analogous procedure (see SI).

Compound [2a]BAr_F. In a Young NMR tube, a solution of complex **[1a]BAr_F** (20 mg, 0.014 mmol) in CD_2Cl_2 (0.5 mL) was treated with H_2 (1 atm). After 5 h at room temperature ^1H NMR analysis of the reaction mixture revealed transformation into complex **[2a]BAr_F** in ≥ 95 % spectroscopic yield. IR (Nujol): $\nu(\text{NH})$ 3426 cm^{-1} . ^1H NMR (CD_2Cl_2 , 25 °C): $\delta = 7.52, 6.57, 6.13$ (t, d, d, 1 H each, $^3J_{\text{HH}} \sim 7.5$ Hz, 3 CH_{Pyr}), 7.37, 7.11, 6.50 (m, d, t, 1 H each, $^3J_{\text{HH}} \sim 7.5$ Hz, 3 $\text{CH}_{\eta^6\text{-Xyl}}$), 7.27 (br d, 3 H, $^3J_{\text{HH}} \sim 7.5$ Hz, 3 CH_{Dipp}), 6.00 (br s, 1 H, NH), 3.18 (sept, 2 H, $^3J_{\text{HH}} \sim 6.5$ Hz, 2 CH_{iPr}), 3.00 (br s, 1 H, CHMe), 2.12 (br s, 6 H, 2 $\text{Me}_{\eta^6\text{-Xyl}}$), 2.06, 1.47 (s, 6 H each, 4 $\text{Me}_{\eta^4\text{-Cyclopentadiene}}$), 1.16 (d+d, 12 H, $^3J_{\text{HH}} \sim 6.5$ Hz, 4 Me_{iPr}), 0.56 (d, 3 H, $^3J_{\text{HH}} \sim 6.5$ Hz, CHMe). $^{13}\text{C}\{^1\text{H}\}$ NMR (CD_2Cl_2 , 25 °C): $\delta = 160.1, 151.1$ ($\text{C}_{\text{q-Pyr}}$), 148.2, 136.3 ($\text{C}_{\text{q-Dipp}}$), 139.2, 114.7, 100.8 (CH_{Pyr}), 129.0, 128.0, 103.0 (CH_{Xyl}), 124.8, 115.2 (2:1, $\text{C}_{\text{q-}\eta^6\text{-Xyl}}$), 102.8, 79.8 (d, $^1J_{\text{CRh}} = 10$ Hz, $\text{C}_{\text{q-}\eta^4\text{-Cyclopentadiene}}$), 59.7 (CHMe), 29.1 (CH_{iPr}), 23.8 (Me_{iPr}), 23.2 (CHMe), 18.5 ($\text{Me}_{\eta^6\text{-Xyl}}$), 14.0, 11.6 ($\text{Me}_{\eta^4\text{-Cyclopentadiene}}$). HRMS (FAB): m/z calcd for $\text{C}_{35}\text{H}_{46}\text{N}_2\text{Rh} [\text{M}]^+$: 597.2716. Found: 597.2682.

Compound [2b]BAr_F. Following the procedure described above, complex [2b]BAr_F was obtained after 24 h in 85 % spectroscopic yield, and it was crystallized from CH₂Cl₂-pentane mixtures at -23 °C. ¹H NMR (CD₂Cl₂, 25 °C): δ = 7.44, 6.46, 6.17 (t, d, d, 1 H each, ³J_{HH} ~ 7.5 Hz, 3 CH_{Pyr}), 7.08 (s, 3 H, 3 CH_{Xyl}), 6.39, 6.01 (t, d, 1:2, ³J_{HH} ~ 6.5 Hz, 3 CH_{η⁶-Xyl}), 5.93 (br s, 1 H, NH), 2.78 (q, 1 H, ³J_{HH} ~ 6.5 Hz, CHMe), 2.15 (s, 6 H, 2 Me_{Xyl}), 1.94 (s, 6 H, 2 Me_{η⁶-Xyl}), 1.95, 1.32 (s, 6 H each, 4 Me_{η⁴-Cyclopentadiene}), 0.43 (d, 3 H, ³J_{HH} = 6.3 Hz, CHMe). ¹³C NMR (CD₂Cl₂, 25 °C): δ = 159.2, 151.5 (C_{q-Pyr}), 139.6, 115.3, 107.8 (CH_{Pyr}), 137.8, 129.7 (2:1, C_{q-Xyl}), 129.5 (CH_{Xyl}), 124.3, 115.4 (1:2, C_{q-η⁶-Xyl}), 103.3, 101.2 (s, d, 1:2, ¹J_{CRh} = 4 Hz, CH_{η⁶-Xyl}), 103.2, 80.2 (d, ¹J_{CRh} ~ 10 Hz, C_{q-η⁴-Cyclopentadiene}), 59.9 (CHMe), 23.8 (CHMe), 19.0 (Me_{η⁶-Xyl}), 18.9 (Me_{Xyl}), 14.4, 12.0 (Me_{η⁴-Cyclopentadiene}). Anal. Calcd (%) for C₆₃H₅₀BF₂₄N₂Rh: C, 53.9; H, 3.6; N, 2.0. Found: C, 53.5; H, 3.8; N, 2.1.

The generation of the related complexes [2c]BAr_F and [2d]BAr_F is detailed in the accompanying SI.

Compound [3a]BAr_F. *Method a:* In a Young NMR tube, a solution of complex [1a]BAr_F (0.04 g, 0.03 mmol) in CH₂Cl₂ (0.5 mL) was treated with H₂ (200 mol %). After 24 h at room temperature ¹H NMR analysis of the reaction mixture revealed transformation into complex [3a]BAr_F in 6% spectroscopic yield.

Method b: In a Young NMR tube, a solution of complex [2a]BAr_F in CD₂Cl₂ (0.5 mL) was heated at 50 °C for 36 h. ¹H NMR analysis of the reaction mixture revealed the formation of complex [3a]BAr_F in 60 % spectroscopic yield.

¹H NMR (CD₂Cl₂, 25 °C): δ = δ 7.5-6.0 (9 CHAr), 5.82 (br s, 1 H, NH), 3.72, 2.50 (d, 1 H each, ²J_{HH} ~ 3.5 Hz, Rh-CH₂), 3.19, 2.81 (sept, 1 H each, ³J_{HH} ~ 6.5 Hz, 2 CH_{iPr}), 2.49 (s, 3 H, 1 Me_{Xyl}), 1.54 (s, 15 H, 5 Me_{Cp*}), 1.32 (d, 3 H, ³J_{HH} ~ 6.5 Hz, 1 Me_{iPr}), 1.27 (m, 6 H, 2 Me_{iPr}), 1.02 (d, 3 H, ³J_{HH} ~ 6.5 Hz, 1 Me_{iPr}). ¹³C NMR (CD₂Cl₂, 25 °C): δ = 96.7 (d, ¹J_{CRh} = 7.3 Hz, C_{q-Cp*}), 47.3 (d, ¹J_{CRh} = 14 Hz, Rh-CH₂), 29.6, 28.8 (1:1, CH_{iPr}), 25.7, 23.8, 23.7, 23.1 (1:1:1:1, Me_{iPr}), 20.7 (Me_{Xyl}), 9.6 (Me_{Cp*}). Other resonances have not been identified in the reaction mixture. HRMS (ESI): m/z calcd for C₃₅H₄₄N₂Rh [M]⁺: 595.2554. Found: 595.2547.

Complexes [3b]BAr_F-[3d]BAr_F were also generated by *Methods a* and *b* detailed above. Please, see SI for details.

ASSOCIATED CONTENT

Supporting Information. X-ray crystallographic data in CIF format, experimental procedures, crystallographic data, and details of the structure determinations for **1a·Cl**, **1b·Cl**, **[1b]BAr_F**-**[1d]BAr_F**, **[1a·CNXyl]BAr_F**, **[1a·(CO)₂]BAr_F**, **[1b·(CO)₂]BAr_F**, **[2b]BAr_F**. This material is available free of charge via the Internet at <http://pubs.acs.org>.

AUTHOR INFORMATION

Corresponding Author

*E-mail: nuria@iiq.csic.es (N. R.), guzman@us.es (E. C.)

Notes

The authors declare no competing financial interest.

ACKNOWLEDGMENT

Financial support (FEDER contribution and ESF) from the Spanish Ministry of Science (projects CTQ2013-42501-P) and the Junta de Andalucía (grant FQM-119 and project P09-FQM-5117) is acknowledged. N. R. thanks the Spanish Ministry of Science and the University of Seville for a “Ramón y Cajal” contract.

REFERENCES

- (1) (a) Bergman, R. G. *Nature* **2007**, *446*, 391–393. (b) Klei, S. R.; Golden, J. T.; Burger, P.; Bergman, R. G. *J. Mol. Cat.* **2002**, *189*, 79–84. (c) Tellers, D. M.; Yung, C. M.; Arndtsen, B. A.; Adamson, D. R.; Bergman, R. G. *J. Am. Chem. Soc.* **2002**, *124*, 1400–1410. (d) Arndtsen, B. A.; Bergman, R. G. *Science* **1995**, *270*, 1970–1973. (e) Burger, P.; Bergman, R. G. *J. Am. Chem. Soc.* **1993**, *115*, 10462–10463.

(2) (a) Hartwig, J. F.; Cook, K. S.; Hapke, M.; Incarvito, C. D.; Fan, Y.; Webster, C. E.; Hall, M. B. *J. Am. Chem. Soc.* **2005**, *127*, 2538–2552. (b) Jones W. D. *Inorg. Chem.* **2005**, *44*, 4475–4484. (c) Jones, W. D.; Feher, F. J. *Acc. Chem. Res.* **1989**, *22*, 91–100.

(3) (a) Taw, F. L.; Mellows, H.; White, P. S.; Hollander, F. J.; Bergman, R. G.; Brookhart, M. Heinekey, D. M. *J. Am. Chem. Soc.* **2002**, *124*, 5100–5108. (b) Wu, X.; Xiao, J. *Chem. Commun.* **2007**, 2449–2466. (c) Daugulis, O.; Brookhart, M. *Organometallics* **2004**, *23*, 527–534. (d) Corberan, R.; Sanau, M.; Peris, E. *J. Am. Chem. Soc.* **2006**, *128*, 3974–3979. (e) Prades, A.; Corberan, R.; Poyatos, M.; Peris, E. *Chem. Eur. J.* **2009**, *15*, 4610–4613. (f) Meredith, J. M.; Goldberg, K. I.; Kaminsky, W.; Heinekey, D. M. *Organometallics* **2009**, *28*, 3546–3551. (g) Ciancaleoni, G.; Bolaño, S.; Bravo, J.; Peruzzini, M.; Gonsalvi, L.; Macchioni, A. *Dalton Trans.* **2010**, *39*, 3366–3368.

(4) (a) Liu, J.; Wu, X.; Iggo, J. A.; Xiao, J. *Coord. Chem. Rev.* **2008**, *252*, 782–809. (b) Goldberg, K. I.; Goldman, A. S. *Activation and Functionalization of C–H Bonds*; Goldberg, K. I., Goldman, A. S., Eds.; ACS: Washington, DC, 2004; pp 1–43. (c) Han, Y.-F.; Jin, G.-X. *Chem. Soc. Rev.* **2014**, *43*, 2799–2823. (d) Dobereiner, G. E.; Crabtree, R. H. *Chem. Rev.* **2010**, *110*, 681–703. (e) Balcells, D.; Clot, E.; Eisenstein, O. *Chem. Rev.* **2010**, *110*, 749–823. (f) Song, G.; Wang, F.; Li, X. *Chem. Soc. Rev.* **2012**, *41*, 3651–3678. (g) Ackermann, L. *Chem. Rev.* **2011**, *111*, 1315–1345.

(5) Liu, Z. Sadler, P. J. *Acc. Chem. Res.* **2014**, *47*, 1174–1185.

(6) (a) Ringenberg, M. R.; Rauchfuss, T. B. *Eur. J. Inorg. Chem.* **2012**, 490–495. (b) Watanabe, M.; Kashiwame, Y.; Kuwata, S.; Ikariya, T. *Eur. J. Inorg. Chem.* **2012**, 504–511. (c) Wang, C.; Villa-Marcos, B.; Xiao, J. *Chem. Commun.* **2011**, *47*, 9773–9785. (d) Kuwata, S.; Ikariya, T. *Dalton Trans.* **2010**, *39*, 2984–2992.

(7) (a) Poli, R. *Chem. Rev.* **1991**, *91*, 509–551. (b) White, C.; Yates, A.; Maitlis, P. M.; Heinekey, D. M. *Inorg. Synth.* **1992**, *29*, 228–234.

(8) (a) Campos, J.; Espada, M. F.; López-Serrano, J.; Carmona, E. *Inorg. Chem.* **2013**, *52*, 6694–6704. (b) Campos, J.; López-Serrano, J.; Álvarez, E.; Carmona, E. *J. Am. Chem. Soc.* **2012**, *134*, 7165–7175. (c) Campos, J.; Esqueda, A. C.; López-Serrano, J.; Sánchez, L.; Cossio,

F. P.; Cozar, A.; Álvarez, E.; Maya, C.; Carmona, E. *J. Am. Chem. Soc.* **2010**, *132*, 16765–16767. (d) Rubio, M.; Campos, J.; Carmona, E. *Org. Lett.* **2011**, *13*, 5236–5239. (e) Campos, J.; Álvarez, E.; Carmona, E. *New. J. Chem.* **2011**, *35*, 2122–2129. (f) Espada, M. F.; Poveda, M. L.; Carmona, E. *Organometallics* **2014**, *33*, 7164–7175. (g) Campos, J. Carmona, E. *Organometallics*, Article ASAP. DOI: 10.1021/om500910t.

(9) (a) Barr, D.; Clegg, W.; Mulvey, R. E.; Snaith, R. *J. Chem. Soc., Chem. Commun.* **1984**, 469–470. (b) Scott, N. M.; Schareina, T.; Tok, O.; Kempe, R. *Eur. J. Inorg. Chem.* **2004**, 3297–3304. (c) Scott, N. M.; Kempe, R. *Eur. J. Inorg. Chem.* **2005**, 1319–1324. (d) Kretschmer, W. P.; Meetsma, A.; Hessen, B.; Schmalz, T.; Qayyum, S.; Kempe, R. *Chem. Eur. J.* **2006**, *12*, 8969–8978. (e) Lyubov, D. M.; Döring, C.; Ketkov, S. Y.; Kempe, R.; Trifonov, A. A. *Chem. Eur. J.* **2011**, *17*, 3824–3826.

(10) (a) Zamorano, A.; Rendón, N.; López-Serrano, J.; Valpuesta, J. E. V.; Álvarez, E.; Carmona, E. *Chem. Eur. J.* **2015**, *21*, 2576–2587. (b) Valpuesta, J. E. V.; Rendón, N.; López-Serrano, J.; Poveda, M. L.; Sánchez, L.; Álvarez, E.; Carmona, E. *Angew. Chem. Int. Ed.* **2012**, *51*, 7555–7557.

(11) See for example: (a) Blacker, A. J.; Clot, E.; Duckett, S. B.; Eisenstein, O.; Grace, J.; Nova, A.; Perutz, R. N.; Taylor, D. J.; Whitwood, A. C. *Chem. Commun.* **2009**, 6801–6803. (b) Nova, A.; Taylor, D. J.; Blacker, A. J.; Duckett, S. B.; Perutz, R. N.; Eisenstein, O. *Organometallics* **2014**, *33*, 3433–3442. (c) Ishiwata, K.; Kuwata, S.; Ikariya, T. *J. Am. Chem. Soc.* **2009**, *131*, 5001–5009.

(12) Spannenberg, A.; Oberthür, M.; Noss, H.; Tillack, A.; Kempe, R. *Angew. Chem. Int. Ed.* **1998**, *37*, 2079–2082.

(13) (a) Heiden, Z. M.; Rauchfuss, T. B. *J. Am. Chem. Soc.* **2009**, *131*, 3593–3600. (b) Heiden, Z. M.; Gorecki, B. J.; Rauchfuss, T. B. *Organometallics* **2008**, *27*, 1542–1549.

(14) (a) Nombel, P.; Lugan, N.; Donnadiou, B.; Lavigne, G. *Organometallics* **1999**, *18*, 187–196. (b) Nonoyama, M. *Inorg. Chim. Acta* **1986**, *115*, 169–172. (c) Nonoyama, M. *Polyhedron* **1985**, *4*, 765–768. (d) Tomon, T.; Koizumi, T.-a; Tanaka, K. *Angew. Chem. Int. Ed.* **2005**, *44*, 2229 –

2232. (e) Adams, C. J.; Baber, R. A.; Connelly, N. G.; Harding, P.; Hayward, O. D.; Kandiah, M.; Orpen, A. G. *Dalton Trans.* **2007**, 1325–1333.

(15) (a) Noyori, R. *Angew. Chem. Int. Ed.* **2002**, *41*, 2008–2022. (b) Sandoval, C. A.; Ohkuma, T.; Utsumi, N.; Tsutsumi, K.; Murata, K.; Noyori, R. *Chem. Asian J.* **2006**, *1*, 102–110. (c) Ohkuma, T.; Utsumi, N.; Tsutsumi, K.; Murata, K.; Sandoval, C.; Noyori, R. *J. Am. Chem. Soc.* **2006**, *128*, 8724–8725.

(16) (a) Liu, T.; Wang, X.; Hoffmann, C.; DuBois, D. L.; Bullock, R. M. *Angew. Chem. Int. Ed.* **2014**, *53*, 5300–5304. (b) Simmons, T. R.; Artero, V. *Angew. Chem. Int. Ed.* **2013**, *52*, 6143–6145. (c) Letko, C. S.; Heiden, Z. M.; Rauchfuss, T. B.; Wilson, S. R. *Inorg. Chem.* **2011**, *50*, 5558–5566. (d) Arita, A. J.; Cantada, J.; Grotjahn, D. B.; Cooksy, A. L. *Organometallics* **2013**, *32*, 6867–6870.

(17) (a) Tejel, C.; Asensio, L.; del Río, M. P.; de Bruin, B.; López, J. A.; Ciriano, M. A. *Eur. J. Inorg. Chem.* **2011**, 512–519. (b) Tejel, C.; del Río, M. P.; Asensio, L.; van den Bruele, F. J.; Ciriano, M. A.; Tschlis i Spithas, N.; Hetterscheid, D. G. H.; de Bruin, B. *Inorg. Chem.* **2011**, *50*, 7524–7534.

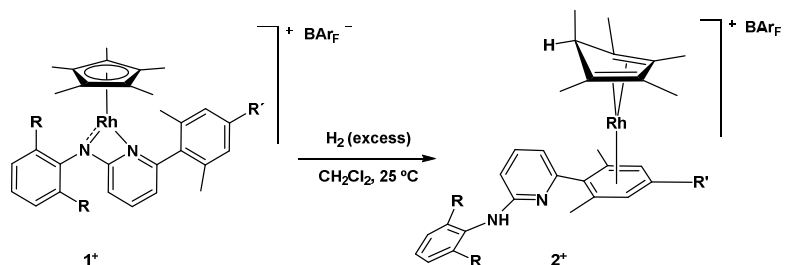
(18) (a) Kang, J. W.; Maitlis, P. M. *J. Organomet. Chem.* **1971**, *30*, 127–133. (b) Umakoshi, K.; Murata, K.; Yamashita, S. *Inorg. Chim. Acta* **1991**, *190*, 185–191. (c) Vargaftik, M. N.; Struchkov, Y. T.; Yanovsky, A. I.; Maitlis, P. M. *Mendeleev Commun.* **1993**, 247–249. (d) Ara, I.; Berenguer, J. R.; Eguizábal, E.; Forniés, J.; Lalinde, E.; Martín, A. *Eur. J. Inorg. Chem.* **2001**, 1631–1640. (e) Liu, L.; Zhang, Q.-F.; Leung, W.-H. *Acta Crystallogr.* **2004**, *E60*, m509–m510.

(19) (a) Nishihara, Y.; Deck, K. J.; Shang, M.; Fehlner, T. P.; Haggerty, B. S.; Rheingold, A. L. *Organometallics* **1994**, *13*, 4510–4522. (b) Nishihara, Y.; Deck, K. J.; Shang, M.; Fehlner, T. P. *J. Am. Chem. Soc.* **1993**, *115*, 12224–12225.

(20) Jones, W. D.; Rosini, G. P.; Maguire, J. A. *Organometallics* **1999**, *18*, 1754–1760.

- (21) (a) Jones, W. D.; Maguire, J. A. *Organometallics* **1987**, *6*, 1301–1311. (b) Churchill, M. R. *J. Organomet. Chem.* **1965**, *4*, 258–260. (c) Alcock, N. W. *J. Chem. Soc., Chem. Commun.* **1965**, 177–178.
- (22) See for instance: (a) Uson, R.; Oro, L. A.; Foces-Foces, C.; Cano, F. H.; García-Blanco, S.; Valderrama, M. *J. Organomet. Chem.* **1982**, *229*, 293–304. (b) Uson, R.; Oro, L. A.; Foces-Foces, C.; Cano, F. H.; Vegas, A.; Valderrama, M. *J. Organomet. Chem.* **1981**, *215*, 241–253.
- (23) (a) Cadenbach, T.; Gemel, C.; Schmid, R.; Fischer, R. A. *J. Am. Chem. Soc.* **2005**, *127*, 17068–17078. (b) Hodson, B. E.; McGrath, T. D.; Gordon, F.; Stone, A. *Inorganic Chemistry* **2004**, *43*, 3090–3097. (c) Macías, R.; Holub, J.; Kennedy, J. D.; Štíbr, B.; Thornton-Pett, M.; Clegg, W. *J. Chem. Soc., Dalton Trans.* **1997**, 149–152.
- (24) Chetwynd-Talbot, J.; Grebenik, P.; Perutz, R. N.; Powell, M. H. A. *Inorg. Chem.* **1983**, *22*, 1675–1684.
- (25) Alaimo, P. J.; Bergman, R. G. *Organometallics* **1999**, *18*, 2707–2717.
- (26) (a) Kumaran, E.; Leong, W. K. *Organometallics* **2012**, *31*, 4849–4853. (b) Kumaran, E.; Sridevi, V. S.; Leong, W. K. *Organometallics* **2010**, *29*, 6417–6421.
- (27) Bernskoetter, W. H.; Schauer, C. K.; Goldberg, K. I.; Brookhart, M. *Science* **2009**, *326*, 553–556.
- (28) Brookhart, M.; Grant, B.; Volpe, A. F. *Organometallics* **1992**, *11*, 3920–3922.

Insert Table of Contents Graphic and Synopsis Here



A study on the reactivity of cationic Rh(III) complexes of composition $[(\eta^5\text{-C}_5\text{Me}_5)\text{Rh}(\text{Ap})]^+$ (complexes **1⁺**) with H₂ is reported. The main products result from a stoichiometric hydrogenation of the C₅Me₅ and aminopyridinate ligands to C₅Me₅H and ApH, respectively, with concomitant metal reduction to Rh(I) (complexes **2⁺**). Additionally, a dihydrogen-catalyzed isomerization of the aminopyridinate ligand from the common $\kappa^2\text{-}N,N'$ bidentate coordination to an unusual $\kappa\text{-}N\text{-}\eta^3$ -pseudo-allyl bonding mode (Rh complexes **3⁺**) is observed.